Ser/Thr phospho-regulation by PknB and Stp mediates bacterial quiescence and antibiotic persistence in *Staphylococcus aureus*

Markus Huemer[1], Srikanth Mairpady Shambat[1], Sandro Pereira[1], Lies Van Gestel[1,2], Judith Bergada-Pijuan[1], Alejandro Gómez-Mejia[1], Chun-Chi Chang[1], Clement Vulin[1], Julian Bär[1], Jonathan Dworkin[3], Annelies S. Zinkernagel[1#]

[1] Department of Infectious Diseases, University Hospital Zurich, University of Zurich, Zurich, Switzerland

[2] University of Hasselt (UHasselt), Hasselt, Belgium

[3] Department of Microbiology and Immunology, College of Physicians and Surgeons, Columbia University, New York, USA

Correspondence to: annelies.zinkernagel@usz.ch

Postal address:
Prof. Dr. med. Annelies S. Zinkernagel
Department of Infectious Diseases and Hospital Epidemiology
University Hospital Zurich
Rämistrasse 100
CH-8091 Zürich
Switzerland
Tel.: +41 44 255 12 59

Keywords: *Staphylococcus aureus*, antibiotic persistence, Stp, PknB, phosphoproteome, quiescence;

Abstract

29   *Staphylococcus aureus* colonizes 30 to 50% of healthy adults and can cause a variety of

30   diseases, ranging from superficial to life-threatening invasive infections such as bacteraemia

31   and endocarditis. Often, these infections are chronic and difficult-to-treat despite adequate

32   antibiotic therapy. Most antibiotics act on metabolically active bacteria in order to eradicate

33   them. Thus, bacteria with minimized energy consumption resulting in metabolic quiescence,

34   have increased tolerance to antibiotics. The most energy intensive process in cells – protein

35   synthesis – is attenuated in bacteria entering into quiescence. Eukaryote-like serine/threonine

36   kinases (STKs) and phosphatases (STPs) can fine-tune essential cellular processes, thereby

37   enabling bacteria to quickly respond to environmental changes and to modulate quiescence.

38   Here, we show that deletion of the only annotated functional STP, named Stp, in *S. aureus* leads

39   to increased bacterial lag-phase and phenotypic heterogeneity under different stress challenges,

40   including acidic pH, intracellular milieu and *in vivo* abscess environment. This growth delay

41   was associated with reduced intracellular ATP levels and increased antibiotic persistence.

42   Using phosphopeptide enrichment and mass spectrometry-based proteomics, we identified

43   possible targets of Ser/Thr phosphorylation that regulate cellular processes and bacterial

44   growth, such as ribosomal proteins including the essential translation elongation factor EF-G.

45   Finally, we show that acid stress leads to a reduced translational activity in the *stp* deletion

46   mutant indicating metabolic quiescence correlating with increased antibiotic persistence.

47

One-sentence summary:

49   Phospho-regulation mediates quiescence and antibiotic persistence in *Staphylococcus aureus.*

Main

The Gram-positive bacterium *Staphylococcus aureus* intermittently or permanently colonizes 30-50% of the human population [1,2]. Although *S. aureus* is part of the normal skin microbiota, it is a leading cause of a variety of nosocomial and community-acquired infections [1]. Besides skin and soft tissue infections (SSTI), *S. aureus* can cause severe and life-threatening, invasive infections such as endocarditis, osteomyelitis and bacteraemia [1]. Increasing levels of resistance against multiple antibacterial drugs, including penicillin, methicillin and vancomycin, render these infections difficult to treat and require prolonged treatment and extended hospitalization [3-5].

Additionally, *S. aureus* can survive antibiotic therapy and cause chronic and recurrent infections even while remaining susceptible to antibiotics [6-8]. This phenomenon of antibiotic persistence or heterotolerance, is defined as the ability of a subpopulation of bacteria to survive high concentrations of bactericidal drugs to which they remain fully susceptible [9]. Subpopulations with different levels of tolerance can co-exist within a bacterial population, facilitating survival in changing environments [9,10]. The strategy of bacterial bet hedging via the formation of persister cells in a clonal bacterial population might be advantageous during infection. The actively growing bacteria in a clonal population are mostly responsible for the colonization of the host and a successful infection, while the subpopulation of persisters ensures the survival of the genotype under fluctuating milieus as found in a host and during antibiotic therapy [11].

Bacterial persisters can occur spontaneously in a population or can be triggered by environmental factors such as low pH, starvation, oxidative stress and drugs, e.g., by inducing tolerance-by-lag [12-17]. Signal transduction through reversible protein phosphorylation is a major

2

75 regulatory mechanism that facilitates quick response to environmental changes [18]. In bacteria,

76 so called two-component systems, consisting of a histidine kinase sensor and an associated

77 response regulator [19], are the most common mechanism of signal transduction. However,

78 regulatory phosphorylation on serine, threonine, and tyrosine residues has been identified in

79 prokaryotes [20,21]. In *S. aureus*, the conserved eukaryotic-type serine/threonine kinase STK

80 (alternatively named PknB or Stk1) and the cognate phosphatase Stp impacts bacterial cell

81 signalling, central metabolism [22-24], stress response [24,25], antibiotic resistance [24,26-28] and

82 virulence [26,27,29-31]. Ser/Thr phosphorylation is also involved in the regulation of protein

83 synthesis, the most energy consuming cellular process and both the initiation and elongation

84 phases of translation are downregulated in response to nutrient limitation [32]. For example, in

85 *B. subtilis*, protein synthesis is downregulated by phosphorylation of the elongation factor Tu

86 (EF-Tu), impairing its essential GTPase activity during nutrient limitation and subsequent

87 formation of dormant spores [33].

88

89 Here, we describe the role of the Ser/Thr kinase/phosphatase pair PknB/Stp in regulating

90 growth and antibiotic persistence in *S. aureus*. By analysing colony size heterogeneity as well

91 as growth delays of individual bacterial cells using single-cell microscopy, we show that

92 increased serine/threonine phosphorylation leads to the formation of non-stable small colonies

93 (nsSCs) as well as prolonged bacterial lag-phases after acidic pH-stress and in bacteria derived

94 from murine abscesses. The identified growth delay correlates with an increased survival of the

95 bacteria in subsequent antibiotic challenges. Phosphopeptide enrichment via Fe^{3+}-Immobilized

96 Metal Affinity Chromatography (IMAC) followed by liquid chromatography-mass

97 spectrometry (LC-MS/MS) analysis enabled us to create a detailed map of PknB and Stp targets.

98 Additionally, we identified changes in phosphorylation states, a decrease in translation activity

99 and increased antibiotic tolerance specifically after acidic pH stress. Together, our results

100 advance the understanding on how *S. aureus* can survive antibiotic treatments despite being

3

101   fully susceptible, by identifying phosphorylation targets that lead to reduced protein synthesis

102   and cellular quiescence.

Results

Deletion of *stp* increases colony growth heterogeneity during stress exposure.

S. aureus encounters a variety of pH conditions during infection, e.g., a neutral pH of 7.4 in the bloodstream during bacteraemia or an acidic pH on the skin, intracellularly in phagosomes or in abscesses [34]. We recently demonstrated that so-called non-stable small colonies (nsSCs), whose size is 5 to 10-times smaller than the most common colony type, result from a bacterial growth delay and correlate with the presence of a persister cell subpopulation [13]. Here, we determined the effect of serine/threonine (Ser/Thr) phosphorylation status on *S. aureus* colony growth and bacterial lag-phases by generating isogenic mutants for *stp* and *pknB* in two distinctive wildtype strains, Cowan I (sequence type [ST] 30) and USA300_JE2 (ST8). These were exposed to defined stress in pH-buffered medium (pH 7.4, 5.5 or 4.0) for three days. While we did not identify any significant differences in the proportion of nsSCs between the wildtype strains and their corresponding isogenic mutants at pH 7.4, we found a significantly elevated proportion of nsSCs in the Δ*stp* mutants (13 to 22%) as compared to the wildtype (5 to 14%) and Δ*pknB* (1 to 15%) after exposure to pH 5.5 for three days (**Fig. 1A**). This effect was even more pronounced when bacteria were exposed to pH of 4.0, with nsSCs levels of up to 37% in the Δ*stp* mutants (**Fig. 1A**). Additionally, there was a trend towards reduced nSCs formation in both Cowan I and USA300_JE2 Δ*pknB* after pH 4 exposure, however not statistically significant (**Fig. 1A**). Furthermore, the deletion mutants Δ*stp* and Δ*pknB* did not exhibit any significant differences in their ability to grow under nutrient rich as well as under various pH conditions when compared to wildtype parent (**Fig. S1, S2A+B**).

Exposure to conditions representative of the intracellular milieu, such as acidic pH, can induce the formation of nsSCs with levels increasing over time [35,36]. To evaluate whether the mutant lacking Stp displays an increased colony size heterogeneity under more complex stress conditions, we infected human lung epithelial cells (A549) with Cowan I and its isogenic

5

128   mutant strains. Cowan I strain elicited significantly less cytotoxicity towards epithelial cells as

129   compared to the haemolytic USA300 strains, hence was utilized for the intracellular stress

130   assay (**Fig. S3**). We monitored the formation of nsSCs over time 3, 5 and 7 days post infection

131   (p.i.) and found that the Δ*stp* mutant strain formed a significantly higher proportion of nsSCs

132   after 5 and 7 days p.i. as compared to its wildtype or Δ*pknB* counterparts (**Fig. 1B**)*.* In contrast,

133   the kinase deletion mutant Δ*pknB* showed a reduction in nsSCs formation over time as

134   compared to both wildtype and Δ*stp* (**Fig. 1B**)*.* None of the mutants displayed a significantly

135   increased or decreased ability to survive intracellularly, but with a trend towards a reduced

136   capacity to survive intracellularly for Δ*pknB* when compared to the wildtype and Δ*stp* for day

137   5 and 7 p.i. (**Fig. S2C**). Together, our data suggest that both the phosphatase Stp and the kinase

138   PknB play a role in the *S. aureus* stress response and influence bacterial growth during different

139   stress conditions.
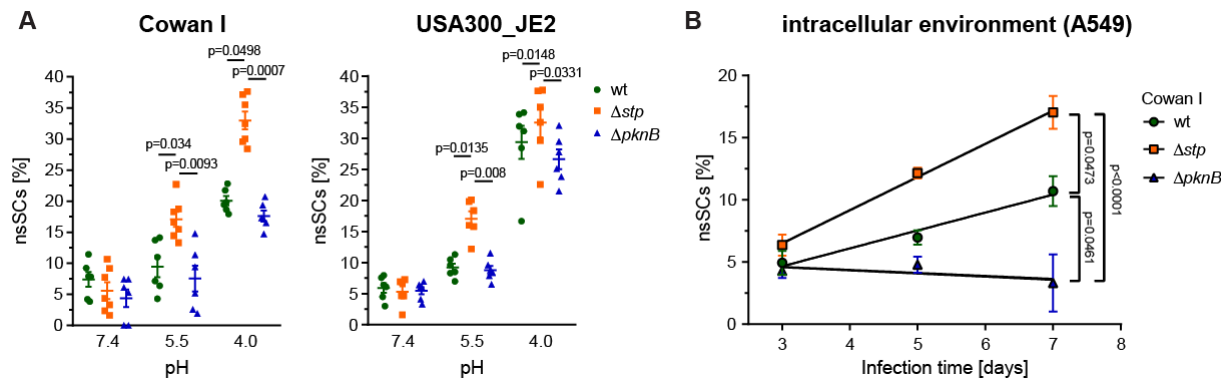
Figure 1: Deletion of *stp* leads to increased formation of nsSCs in *S. aureus* after different stress exposures. A) Proportion of nsSCs in *S. aureus* strains Cowan I and USA300_JE2 after three days of pH 7.4, 5.5 or 4.0 exposure. N= 6 to 7 biological replicates. **B)** Proportion of nsSCs in *S. aureus* strain Cowan I after exposure to the intracellular environment of human lung epithelial cells (A549) for 3, 5 and 7 days. Statistically significant p-values are displayed. Statistical significance was determined by the Kruskal-Wallis test with Dunn`s post-test. Error bars depict standard error of mean (SEM).

**Growth-resumption delays and reduced ATP-levels in Δ*stp* after acid stress.**

To verify that the proportion of nsSCs reflects the growth-delay of individual bacterial cells, we determined the time single bacterial cells needed to start their first cell division after changing to favourable growth conditions using time lapse microscopy. The lag-phase was assessed for pH 5.5-exposed bacteria as well as for exponential phase bacteria that served as a control (**Fig. 2A, S4**). While exponentially growing bacteria did not exhibit differences (**Fig. S4**), the lag-phase of mutants after acid stress changed significantly, as expected from our persister measurements on nsSCs (**Fig. 2A**). We observed growth delays of up to 12 h for Cowan I Δ*stp* and 10 h for USA300_JE2 Δ*stp*. The wildtype strains showed lag-phases of up to 8 h for Cowan I and 4 h for USA300_JE2. While there was no significant difference in the lag-phases between the wildtype and Δ*pknB* in Cowan I (90% of the bacteria have started to grow after 5.5 h), USA300_JE2 Δ*pknB* had a significantly reduced lag-phase as compared to its wildtype counterpart after pH 5.5 exposure (**Fig. 2A**).

7

162 To determine whether the growth delay is linked to reduced energy levels, we measured

163 intracellular ATP concentrations of the bacteria after exposure to acidic pH (**Fig. 2B**). We found

164 that the Δ*stp* mutant, which showed significantly prolonged bacterial lag-phases after pH 5.5-

165 exposure (**Fig. 2A**), displayed significantly lower ATP levels (50% reduction) as compared to

166 the wildtype and Δ*pknB* mutant in both Cowan I and USA300_JE2 (**Fig. 2B**). Slightly, but

167 significantly reduced ATP levels were found for Cowan Δ*pknB* as compared to the wildtype,

168 while there was no difference between USA300_JE2 wildtype as compared to Δ*pknB*. These

169 findings are consistent with previously published metabolomics data showing significantly

170 reduced ATP levels in stationary *S. aureus* strain 8325 Δ*stp*, but not in Δ*pknB* [37]. Our data show

171 that, in the absence of Stp, the single cell growth delay after acid stress is associated with

172 reduced intracellular ATP levels.

173

174 **Delays in growth resumption and reduced ATP levels contribute to antibiotic persistence.**

175 To determine if high proportions of late-growing bacteria with reduced ATP levels are

176 associated with increased antibiotic persistence, we challenged acidic pH-exposed wildtype

177 strains of *S. aureus* as well as their deletion mutants Δ*stp* and Δ*pknB* with high concentrations

178 of antibiotics (40x the minimum inhibitory concentration [MIC]). To test the survival capacity

179 of Cowan I, we used the cell wall targeting antibiotic flucloxacillin (FLU), the DNA-replication

180 inhibitor fluoroquinolone ciprofloxacin (CIP) and the transcription inhibitor rifampicin (RIF).

181 For USA300_JE2, we used the cell wall targeting drugs FLU and vancomycin (VAN) as well

182 as RIF.
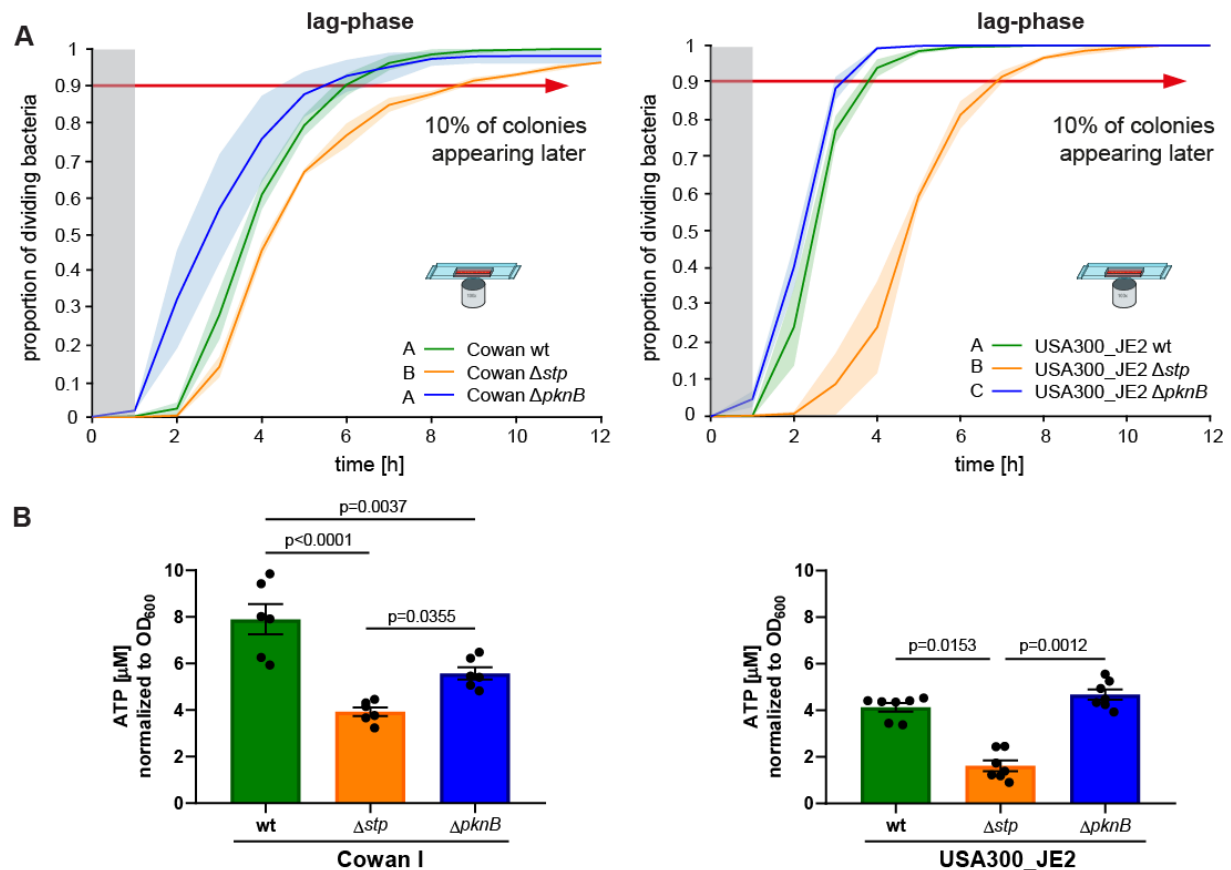
Figure 2: Acidic pH-exposure increases bacterial lag-phase and results in reduced ATP levels in S. aureus Δstp. A) Single-cell microscopy of *S. aureus* wildtype and the isogenic mutants Δ*stp* and Δ*pknB* growing in nutrient-rich medium after three days of pH 5.5 exposure. N= 3 biological replicates. Shaded areas depict the standard deviation. Cowan I wt pH 5.5 n= 475 bacterial cells, Cowan I Δ*stp* pH 5.5 n= 246, Cowan I Δ*pknB* pH 5.5 n= 554; USA300_JE2 wt pH 5.5 n= 662 bacterial cells, USA300_JE2 Δ*stp* pH 5.5 n= 669, USA300_JE2 Δ*pknB* pH 5.5 n= 1,062; Grey zone marks the period at the beginning of the experiment, where cell divisions could occur, but would not be observed. Letters indicate statistically significantly different groups. Statistical significance was determined for the time points where 90% of the bacteria started to divide (red arrow). **B)** *S. aureus* was grown in DMEM pH 5.5 for three days. Intracellular ATP concentration was determined using a BacTiter-Glo cell viability assay. N= 6 biological replicates. Statistically significant p-values are displayed; Statistical significance was determined by one-way ANOVA with Tukey post-test after passing the Shapiro-Wilk normality test. Error bars depict SEM.

198   Consistent with the increased bacterial lag-phase and the reduced ATP levels in the Δ*stp*

199   mutants of both strains after pH 5.5-exposure (see **Fig. 1+2**), we observed increased levels of

200   antibiotic tolerance towards several different antibiotics (**Fig. 3A-D**). Calculating the minimum

201   duration for killing 90% of the initial bacterial population (MDK_{90}) for FLU and CIP as well

202   as the MDK_{99} for the rapidly acting antibiotic RIF for Cowan I (**Fig. 3B**) and MDK_{90} for FLU,

203   VAN and RIF for USA300_JE2 (**Fig. 3D**) allowed us to better compare between strains and

204   treatments. We found that 90% of the initial population of pH 5.5-exposed Cowan Δ*stp* was

205   killed by FLU after 19 h, whereas it took only 6 h for the wildtype and 5 h for Δ*pknB*. A similar

206   pattern was revealed for CIP and RIF (**Fig. 3B**). Analogously, a similar behaviour was identified

207   for USA300_JE2 challenged with FLU, VAN or RIF (**Fig. 3D**). To exclude resistance

208   development as a confounding factor for RIF persistence, we additionally plated on RIF-plates

209   and excluded experiments where resistance development occurred from this analysis (**Fig. S5**).

10
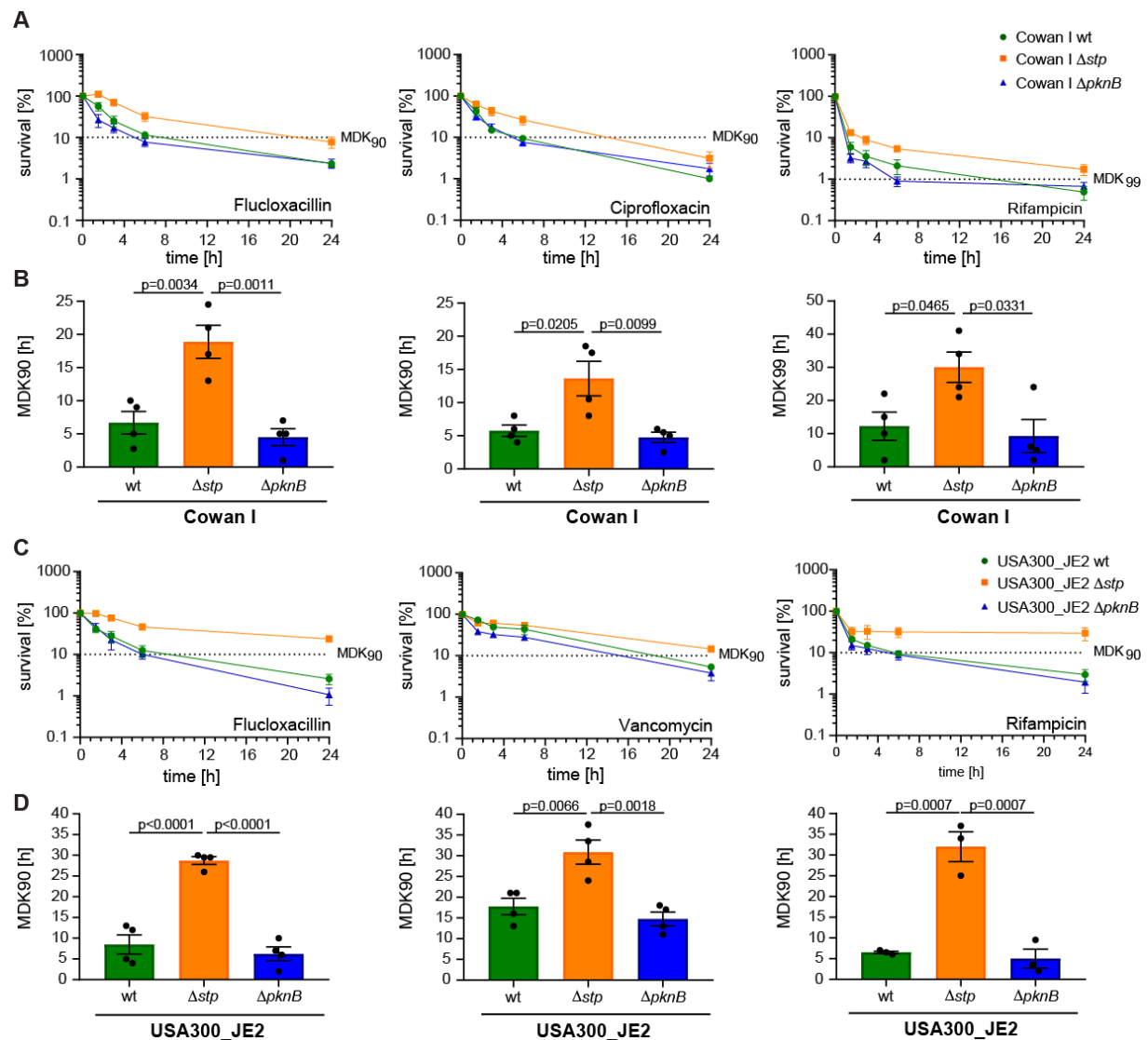
Figure 3: Increased antibiotic tolerance in Δ*stp* after acidic pH-exposure. A-D) *S. aureus* was grown in DMEM pH 5.5 for three days before inoculation in neutral pH medium supplemented with antibiotics (40xMIC) as indicated. **A+C**) Time kill curves (0, 1.5, 3, 6 and 24 h) for different antibiotics and strains (Cowan I and USA300_JE2). To determine bacterial survival, bacteria were sampled at different time points, washed three times to eliminate antibiotics and plated for CFU enumeration. Survival was calculated relative to the initial inoculum of ~10^5 CFUs/ml. **B+D**) Minimum duration of killing 90 or 99% of the initial population for different strains and antibiotics. Statistically significant p-values are depicted. Statistical significance was determined by one-way ANOVA with Tukey´s multiple comparison testing after passing the Shapiro-Wilk normality test. Error bars depict SEM.

11

221 **_stp_ deletion leads to increased bacterial lag-phase and antibiotic persistence in mice.**

222 To test whether the _stp_ deletion leads to increased bacterial lag-phases and a subpopulation of

223 persisters _in vivo_, we infected mice with either _S. aureus_ wildtype or the corresponding isogenic

224 mutants Δ_stp_ and Δ_pknB_ (**Fig. 4A**). Here, we used the less cytotoxic Cowan I to induce abscess

225 formation and pus production in the mice as described previously [13,38]. Five days post-infection,

226 mice were sacrificed, abscess size measured, and the pus harvested for further analysis. The

227 Δ_stp_ strain caused significantly larger abscesses compared to Δ_pknB_, but there was no

228 significant difference between the wildtype and Δ_stp_ as well as wildtype and Δ_pknB_ (**Fig. S6A**).

229 Analysis of the colony growth heterogeneity showed that Δ_stp_ formed a higher proportion of

230 nsSCs (up to 13%) as compared to both wildtype (up to 5.9%) and Δ_pknB_ (up to 4.8%),

231 indicating the presence of a larger quiescent subpopulation in the absence of Stp in _in vivo_

232 abscess settings (**Fig. 4B, S6B+C**). Single cell microscopy confirmed prolonged individual

233 bacterial lag-phases in Δ_stp_ as reflected by the increased proportion of nsSCs (**Fig. 4C**). To test

234 whether _S. aureus_ lacking the phosphatase Stp not only forms larger abscesses and more nsSCs,

235 but also a larger subpopulation of persister cells, we exposed bacteria isolated from murine

236 abscesses to high concentrations of FLU and CIP (40xMIC) for 24 h and analysed their survival

237 capacity (**Fig. 4D**). We found that the Δ_stp_ mutant showed significantly higher survival levels

238 (up to 16%) as compared to the wildtype (up to 6%), correlating with the increased proportion

239 of nsSCs (**Fig. 4E, S6D+E**). Additionally, the kinase mutant Δ_pknB_ showed reduced antibiotic

240 persistence; we found significantly lower survival in FLU as compared to both wildtype and

241 Δ_stp_ as well as a trend to lower survival compared to the wildtype in CIP (**Fig. 4D**). Together,

242 our data demonstrate that the kinase/phosphatase pair PknB/Stp modulates antibiotic

243 persistence in _S. aureus in vivo_, and that a lack of Ser/Thr dephosphorylation can lead to an

244 increased subpopulation of persisters.

12
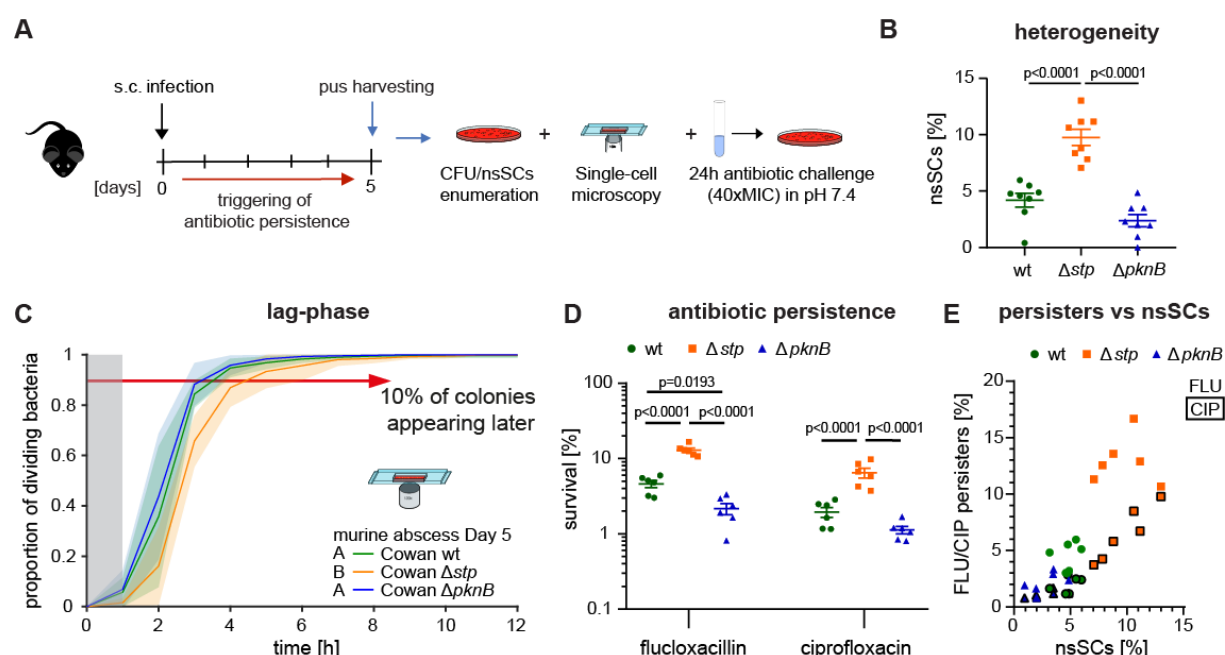
Figure 4: Deletion of *stp* leads to increased bacterial lag-phase and antibiotic persistence in mice.
A) Scheme of the murine infection model. **B**) Colony size heterogeneity in murine abscess pus. Proportion of nsSCs was calculated relative to total CFU (**Fig. S6B+C**). Statistical significance was determined by one-way ANOVA with Tukey´s multiple comparison testing. **C**) Single cell microscopy to determine individual cells' lag-phases after recovery from murine abscess pus. Cowan I wildtype n= 727 bacterial cells; Cowan I Δstp n= 1,038 and Cowan I $\Delta pknB$ n= 776; Grey zone marks the period at the beginning of the experiment where cell divisions could occur but would not be observed. Letters indicate statistically significantly different groups. **D**) Survival assay of bacteria harvested from murine abscesses and exposed to FLU or CIP for 24 h. Survival was calculated relative to the initial inoculum. Statistical significance was determined by a two-way ANOVA with Tukey´s multiple comparison testing after passing the Shapiro-Wilk normality test. **E)** Relationship between the proportion of nsSCs and the proportion of persisters (FLU= no border, and CIP= black boarder colour). Each symbol represents one murine abscess. **B-E)** N= 6 abscesses from 3 mice. Error bars depict SEM.

13

259 **Phosphoproteomic analysis reveals protein synthesis as a target of PknB and Stp during**

260 **acid stress.**

261 To elucidate the role of Ser/Thr phosphorylation in *S. aureus* antibiotic persistence and growth

262 regulation, and to further identify potential down-stream targets of PknB and Stp, we performed

263 total proteome as well as phosphoproteomic analyses on pH 5.5 exposed strain Cowan I wt and

264 its respective *pknB* and *stp* deletion mutants (**Fig. 5A**). As previously reported [39], *S. aureus*

265 favours single phosphorylated peptides, with over 80% of identified peptides phosphorylated

266 only once. However, deletion of Stp led to an increased number of single and double

267 phosphorylated peptides, while deletion of *pknB* showed no drastic differences when compared

268 to the wildtype (**Fig. S7A**), suggesting the presence of additional Ser or Thr kinases in *S. aureus*.

269 Similarly, a heatmap overview of all identified phosphopeptides (**Fig. 5B**) showed a similar

270 pattern in wildtype and Δ*pknB,* with only 33 significantly underrepresented and seven

271 overrepresented phosphopeptides in Δ*pknB* as compared to wildtype (**Fig. S7B**, *right panel*,

272 and **D**). A prominent difference in phosphopeptides was revealed between Δ*stp* and wildtype,

273 with 240 phosphopeptides significantly overrepresented (90% on Thr) and 137 significantly

274 underrepresented (55.5% on Ser) (**Fig. 5C,** *right panel,* and **S7B**). On the entire proteome level,

275 1,550 proteins (coverage of 59.5%) were identified, of which 2.8% (43 proteins) were

276 differentially expressed. Specifically, 1.5% (23 proteins) were found to be significantly

277 downregulated and 1.3% (20 proteins) significantly upregulated in Δ*stp* as compared to

278 wildtype (**Fig. 5C**, *left panel*). Consequently, most of the changes occurred exclusively on the

279 phosphoproteome and not on the total proteome (**Fig. S7C**), which is in line with previously

280 published data [39]. Phosphorylation of ribosomal proteins such as RplS (pT11), RpsC (pT176)

281 and RpsP (pT70), translation elongation factors EF-Tu (pT34) and EF-G (pT34, pT43 and

282 pT424) and cell division proteins such as FtsZ (pT333, pS338 and pT367) were prominently

283 overrepresented in the *stp* deletion mutant as compared to the wildtype (**Fig. 5C**, *right panel*,

284 and **5D+E**). Deletion of the kinase PknB, on the other hand, showed a similar phosphorylation

14

285   pattern as the wildtype for both ribosomal proteins and the translation elongation factor EF-G

286   (**Fig. S7E**+**F**). Phosphorylation of translation elongation factors has been linked to reduced

287   translational activity and bacterial dormancy in *B. subtilis* [33] and our data shows that

288   phosphorylation of translation elongation factors seems to play an important role in *S. aureus*

289   as well (**Fig. 5**). The increased phosphorylation on several Thr-residues in EF-G, e.g., the

290   sixteen-fold increase for pT43, was confirmed by immunoblotting wherein only in Δ*stp* the

291   antibody signal from EF-G and P-Thr overlapped but did not align in the wildtype nor in Δ*pknB*

292   (**Fig. 5F, S7G**). Similar results were found for *S. aureus* USA300_JE2 (**Fig. S7H**).

293   To assess if the overrepresented phosphorylation of ribosomal and translation elongation factors

294   is associated with differences in protein synthesis activity, we measured incorporation of the

295   puromycin analogue O-propargyl-puromycin (OPP) [40] to monitor protein synthesis in pH 5.5

296   exposed *S. aureus* Cowan I. We found that the *stp* deletion mutant shows significantly reduced

297   protein synthesis activity as compared to the wildtype, while the *pknB* deletion mutant

298   displayed increased protein synthesis (**Fig. 5G**). Taken together, these data suggest that

299   phosphoregulation of proteins involved in translation leads to reduced protein synthesis in

300   *S. aureus* during acid stress exposure.
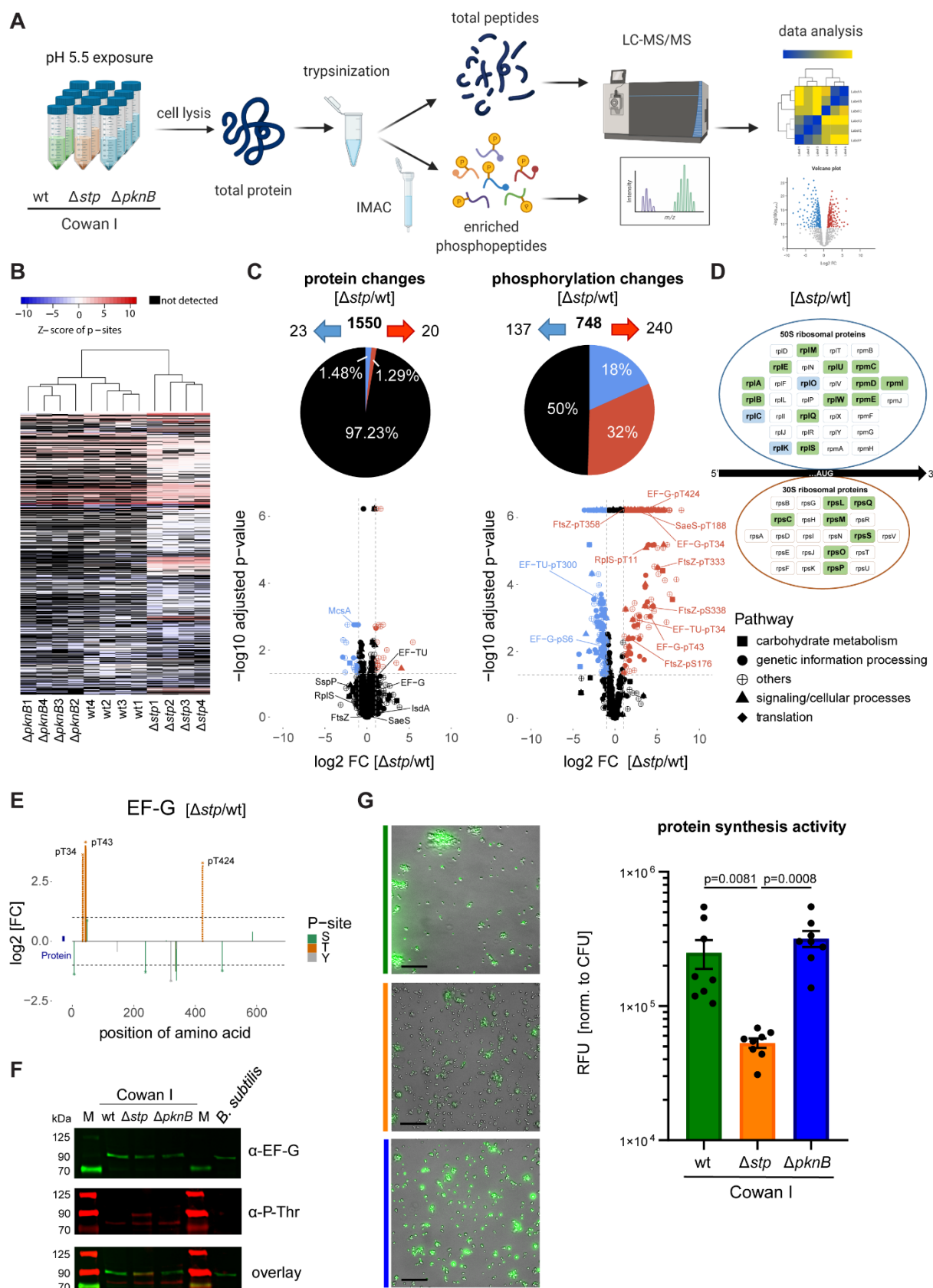
Fig. 5: Phosphorylation and protein expression alterations in acid stress exposed *S. aureus*. A) Experimental workflow for proteomic and phosphoproteomic analysis. After cell lysis to isolate

16

304   bacterial total protein from *S. aureus* strain Cowan I grown at pH 5.5 for three days, total proteome and

305   enriched phospho-peptides were analysed via label-free LC-MS/MS. **B)** Hierarchical cluster analysis of

306   phosphopeptide abundance in phosphoproteome. The abundance profiles of the phosphopeptides in our

307   four replicates hierarchically clustered by heatmap. Blue indicates less abundant phosphopeptides,

308   whereas red indicates more abundant phosphopeptides. Black indicates non-detected phosphopeptides.

309   **C)** Pie charts and volcano plots comparing total proteome (*left panel*) and phosphopeptide (*right panel*)

310   changes between Cowan I *stp* deletion mutant and wildtype, identifying differentially expressed proteins

311   or phosphopeptides (cut-off adjusted p-value < 0.05 and a fold change of $|\log_2 FC| > 1$).

312   Underrepresented proteins/ phosphopeptides are depicted by blue symbols and overrepresented proteins/

313   phosphopeptides with red symbols. Symbol type indicates Kyoto Encyclopedia of Genes and Genomes

314   (KEGG) pathway. **D)** Identified changes in Ser/Thr phosphorylation of ribosomal proteins in Cowan I

315   *stp* deletion mutant compared to its wildtype. Green colour indicates increased Ser/Thr phosphorylation

316   (at least one phospho-site $\log_2 FC \geqq 1$, adjusted p-value < 0.05). Blue colour indicates decreased Ser/Thr

317   phosphorylation (at least one phospho-site $\log_2 FC \leqq -1$, adjusted p-value < 0.05). If upregulated and

318   downregulated phosphopeptides for the same protein were found, the highest up- or downregulation is

319   shown. **E)** P-sites to protein plot for the elongation factor EF-G. Phosphorylation sites and exact amino

320   acid positions are indicated. Y-axis indicates $\log_2$ fold changes of phosphopeptides in Cowan I Δstp

321   compared to wildtype. Dashed lines indicate pseudo fold changes (phosphopeptides were only detected

322   in one condition). **F)** Representative immunoblots of bacterial cell lysates with antibody specific for

323   phospho-threonine and rabbit serum raised against *B. subtilis* EF-G that also recognises *S. aureus*

324   EF-G. Cowan I wildtype, Δstp and $\Delta pknB$ were grown at pH 5.5 for three days, *B. subtilis* was grown

325   to stationary phase for 16 h. **G)** Representative images of OPP-stained Cowan I wildtype, Δstp and

326    $\Delta pknB$. Fluorescence indicates protein synthesis (*left panel*). Total fluorescence of OPP-labelled

327   *S. aureus* normalized to CFUs (*right panel*). Scale bar indicates 20 μm.

Discussion

329 This study shows that the Ser/Thr kinase PknB and its cognate Ser/Thr phosphatase Stp

330 regulates antibiotic persistence in *S. aureus* (as summarized in **Fig. 6**). Measurement of

331 translation showed significantly reduced protein synthesis consistent with increased Ser/Thr

332 phosphorylation after acid stress when the phosphatase Stp is absent. Similarly, deletion of *stp*

333 increases the subpopulation of quiescent bacteria upon stress exposure, which was reflected by

334 elevated levels of nsSCs and by lag-phase analysis of individual bacterial cells using single cell

335 microscopy. Additional analysis revealed decreased levels of intracellular ATP in the Δ*stp*

336 mutant, further indicating a metabolically reduced state of the bacteria. Both *in vitro* acid stress,

337 and *in vivo* stress exposure in murine abscesses lead to increased numbers of bacteria with a

338 high growth delay. Our data show that the growth delay as well as the reduced ATP levels of

339 an Δ*stp* mutant relates to its increased ability to survive high concentrations of antibiotics from

340 different classes. Finally, phosphoproteomic analysis of the *S. aureus* strain Cowan I revealed

341 increased phosphorylation of proteins involved in translation such as ribosomal proteins and

342 translation factors. This highlights the role of phospho-regulation in bacterial quiescence and

343 survival during antibiotic challenges and the interplay between the kinase PknB and the

344 phosphatase Stp (**Fig. 6, S10**).

345 PknB was initially identified in a genetic screen designed to detect factors that regulate

346 methicillin resistance in *S. aureus* [41]. It is highly conserved throughout all sequenced *S. aureus*

347 genomes [22,30,42] and has a domain architecture consisting of extracellular penicillin-binding

348 protein- and STK-associated (PASTA) domains, a transmembrane domain and an intracellular

349 catalytic kinase domain, similar to *B. subtilis* PrkC as well as *M. tuberculosis* PknB [31]. Previous

350 phosphoproteomic studies identified PknB target proteins involved in metabolic processes such

351 as glycolysis, citrate cycle, cell wall synthesis and protein synthesis [23,39,43]. Both PknB and Stp

352 play an important role in cell wall synthesis and it has been shown that deletion of *stp* leads to

353   a thickened and more robust cell wall in *S. aureus* resulting in decreased susceptibility to

354   lysostaphin and vancomycin [27,42-44]. Similarly, we observed a two-fold increase in the MICs for

355   cell wall targeting antibiotics such as flucloxacillin and vancomycin (**Table S3**). However, as

356   we used high antibiotic concentrations for our killing assays, doubled MIC values for ß-lactams

357   do not alone explain the increased survival of the *stp* deletion mutants during ß-lactam

358   challenge.

359   We recently found elevated levels of proteins involved in protein, nucleotide and amino-

360   acid biosynthesis in a persister-enriched population of a clinical isolate of *S. aureus* that was

361   isolated from a difficult-to-treat infection, [38]. Higher levels of PknB might lead to increased

362   phosphorylation levels that in turn can reduce translation, alter cell wall synthesis and can lead

363   to decreased intracellular ATP levels. Inhibition of protein synthesis by phosphorylation of the

364   elongation factor Tu (EF-Tu) in *B. subtilis* has been shown to occur during nutrient limitation

365   and ultimately lead to the formation of dormant spores- an extreme form of bacterial persistence

366   [33]. In *E. coli*, phosphorylation of EF-Tu leads to its inactivation and to the inhibition of protein

367   synthesis during environmental stress such as starvation [45]. In general, inhibition of protein

368   synthesis has been shown to increase antibiotic persistence in *E. coli* [46,47].

369   Here, we show that deletion of *stp* leads to increased Thr phosphorylation (pT34, pT43,

370   pT424) of EF-G and extensive phosphorylation of ribosomal proteins in acid stress exposed

371   *S. aureus*. Together with reduced protein synthesis, low ATP levels and a delayed onset of

372   growth after stress removal, this correlated with increased antibiotic tolerance in *S. aureus*.

373   Also, proteins involved in cell division and bacterial growth were found to be phosphorylated

374   by PknB. For example, the core divisome component FtsZ showed increased phosphorylation

375   in the absence of Stp after acid-stress exposure. Phosphorylation of FtsZ might inhibit its

376   GTPase activity leading to arrested cell division [48,49]. Furthermore, it has been shown that

377   Ser/Thr phosphorylation of FtsZ is important for complex formation with the cell division

378   protein FtsQ in *M. tuberculosis* during oxidative stress, highlighting the importance of Ser/Thr

379   phosphorylation in maintaining bacteria in a division-competent state depending on the growth

380   conditions [50].

381   Bacterial growth delays and cellular quiescence have been linked to antibiotic tolerance

382   and the presence of nsSCs can be indicative of a subpopulation of persister cells [13,51,52]. The

383   increased levels of nsSCs in *S. aureus* lacking Stp and the growth delay observed on the single-

384   cell level are associated with reduced energy levels and increased bacterial survival during

385   antibiotic exposure. Reduced intracellular ATP levels have been linked to antibiotic tolerance

386   as most antibiotics require an active target and bacterial metabolism in order to eradicate

387   bacteria [53-55]. Growth delays, nsSCs as well as antibiotic persistence were not only detected

388   after *in vitro* stress exposure, but also *in vivo* after harvesting bacteria from murine abscesses.

389   Since deletion of the kinase PknB did not completely eliminate Ser/Thr phosphorylation in

390   *S. aureus*, other phospho-donors such as acetyl-phosphate, ammonium hydrogen and

391   carbamoyl phosphate or other currently unknown Ser/Thr kinases [39,56,57] may participate in this

392   response.

393   We generated a comprehensive map of the phosphoproteome of *S. aureus* Cowan I and

394   its isogenic mutant strains exposed to acidic pH linking Ser/Thr phosphorylation to reduced

395   protein synthesis and intracellular ATP levels and thereby increased bacterial survival during

396   antibiotic exposure. The kinase inhibitor staurosporine increases methicillin-resistant *S. aureus*

397   (MRSA) sensitivity to the β-lactam nafcillin [58] suggesting that inhibition of PknB during

398   infection might reduce formation of persister cells. Thus, the kinase/phosphatase pair PknB and

399   Stp may be a future target to prevent persister formation during chronic and difficult-to-treat

400   infections that require prolonged antibiotic therapies.

401
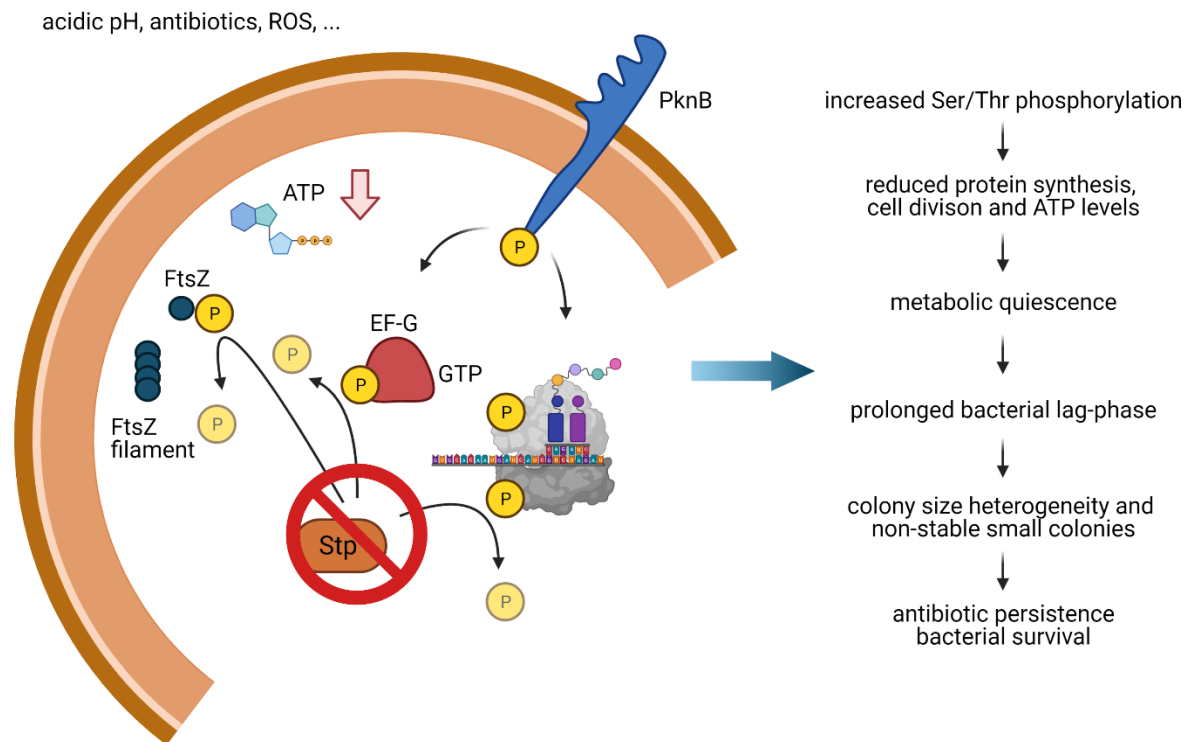
Figure 6: Phosphorylation-changes linked to cellular quiescence and antibiotic persistence in *S. aureus*. Scheme summarizing the results of this study (see **Fig. S10**). Sensing of extracellular stressors by the eukaryote-like Ser/Thr kinase PknB leads to phosphorylation of proteins involved in protein synthesis, cell division and growth in *S. aureus* resulting in reduced protein synthesis, cell division and ATP levels. This metabolic quiescence leads to prolonged bacterial lag-phases and thus to a delayed onset of growth after switching to favourable conditions. This growth delay manifests in the formation of non-stable small colonies (nsSCs) and eventually in colony size heterogeneity on agar plates. Ultimately, *S. aureus* is able to survive antibiotic challenges and shows increased antibiotic persistence. Yellow circles indicate phosphor residues. ATP= adenosine triphosphate, Stp= Ser/Thr phosphatase, EF-G= elongation factor G, FtsZ= core divisome component protein, GTP= guanosine triphosphate; Created with BioRender.com.

Materials and Methods

Bacterial Culture and Growth Conditions.

Bacterial strains used in this study are listed in **Table S1**. *S. aureus* was grown on Columbia agar plates supplemented with 5% sheep blood (BioMérieux) overnight prior to use or on tryptic soy broth (TSB) (Becton Dickinson) containing 1.5% agar (Becton Dickinson) for bacterial enumeration. For exponential growth conditions, bacteria were grown in TSB overnight (16 h) shaking (220 rpm) at 37°C, diluted and regrown in TSB, shaking at 37°C, for two hours. For pH-stress assays, *S. aureus* was inoculated into defined pH media (Dulbecco's Modified Eagle Medium (DMEM) pH 4.0, 5.5 and 7.4) at a starting OD_{600} of 0.2. After incubation at 37°C and 5% CO2 for three days and daily mixing, cultures were analysed by plating and counting nsSCs or by determining antibiotic persistence in a survival assay. NsSCs enumeration was performed as described previously [13]. Specific growth conditions are described in the corresponding method sections.

Genetic manipulations.

For both strains, Cowan I and USA300_JE2, unmarked deletions for either *pknB* or *stp* were created using the pIMAY vector as previously described [59]. Briefly, *S. aureus* strains were transformed with pIMAY containing the modified genomic sequences missing either *pknB* (pSP11; **Fig. S8**) or *stp* (pSP13; **Fig. S9**) by electroporation. Primers and plasmids used to create pSP11 and pSP13 are described in **Table S2**. Colonies grown on tryptic soy broth agar plates supplemented with 10 µg/ml chloramphenicol (Cm), containing the plasmid were used for chromosomal integration by homologous recombination. Deletion of *pknB* and *stp* was confirmed by PCR and sequencing. To rule-out inherent growth defects of the deletion mutants, we performed growth curves and did not identify any differences in growth of the mutants compared to their wildtypes (**Fig. S1**).

439 **Eukaryotic cell infections.**

440 The human lung epithelial carcinoma cell line A549 (ATCC CCL-185) was grown in DMEM

441 4.5 g ml^{-1} glucose (Life Technologies) with 10% foetal bovine serum (FBS; GE- Healthcare)

442 and 2 mM L-glutamine (Life Technologies) and infected with *S. aureus* strain Cowan I at a

443 multiplicity of infection of 1. Three hours after infection, the cells were washed with phosphate-

444 buffered saline (DPBS; Life Technologies), and flucloxacillin (Actavis; 1 mg ml^{-1} in DMEM)

445 and lysostaphin (Sigma; 25 µg ml^{-1} in DMEM) were added to kill any extracellular bacteria.

446 Every day, the washing step was repeated, and fresh medium (containing flucloxacillin

447 1 mg ml^{-1} and lysostaphin 25 µg ml^{-1}) was added to the host cells. Supernatants were monitored

448 for the absence of any extracellular bacteria by plating. Three-, five- and seven-days post-

449 infection, host cells were washed three times with PBS, lysed (0.08% Triton X-100 (Fluka) in

450 PBS), and plated on Columbia agar plates supplemented with 5% sheep blood for nsSCs

451 enumeration.

452

453 **Single-cell time-lapse microscopy.**

454 Agar pads were prepared using a custom-made device made of polyvinyl chloride. Bacterial

455 dilutions were added onto solidified 2% agar (bacteriological grade, BD) with Columbia media

456 (BD) and 5% sheep blood (Life Technologies) and then covered with a cover glass. The setup

457 was then placed under a microscope at 37°C at the latest 30 min after inoculation. Bright field

458 images were acquired using a fully automated Olympus IX81 inverted microscope at 100×

459 resolution (U-FLN-Oil lens) and the Cellsense software. Up to 3,000 positions were monitored

460 per experiments and the lag-phase of 246–2,000 bacteria per strain was analysed [13]. Statistical

461 significance was determined for time points where 90% of bacteria started to divide using

462 unpaired t-tests.

23

Mouse experiment.

The protocols (ZH251/14 and ZH050/18) were approved by the institutional animal care and use committee of the University of Zurich and all experiments were conducted in approval of the Cantonal Veterinary Office Zurich.

S. aureus Cowan I wildtype as well as the isogenic mutants Δ*pknB* and Δ*stp* were grown to logarithmic phase and 10^8 CFUs mixed 1:1 with cytodex beads (Sigma) [60]. Bacteria were injected into the flanks of 7–9-weeks-old female C57BL/6 mice (Janvier Laboratory, France). Mice were sacrificed 5 days post-infection. Abscess area was measured, and abscess volume calculated as previously described [61]. Abscess pus was harvested, homogenized, lysed and directly analysed by single-cell time-lapse microscopy as well as plating serial dilutions for bacterial enumeration and nsSC quantification. Additionally, bacteria from abscess pus were used for subsequent persister assays.

ATP-assay.

Intracellular adenosine triphosphate (ATP) levels were measured using a BacTiter-Glo kit (Promega) according to the manufacturer's instructions. *S. aureus* grown in DMEM supplemented with 10% FBS and 1% L-Glu at pH 5.5 for three days were washed with PBS before measuring luminescence on a SpectraMax i3 MiniMax 300 plate reader (Molecular Devices) in white 96-well flat bottom plates. (Greiner Bio-One). ATP levels were normalized to CFU counts. N= 6 biological replicates.

Persister assay and time kill curves.

Approximately 10^5 bacteria from different stress conditions (pH 5.5 or murine abscess pus) were inoculated in DMEM pH 7.4 supplemented with antibiotics (40xMIC) as indicated. After 1.5 h, 3 h, 6 h and 24 h of incubation at 37°C and 5% CO_2, bacterial survival was determined by CFU enumeration and calculated relative to the inoculum. MICs for FLU, VAN, RIF and CIP were assessed by micro broth dilution method, following the "European Committee for

24

490   Antimicrobial Susceptibility Testing" (EUCAST) recommendations. Minimum duration of

491   killing 90% or 99% of the initial population (MDK90/99) was calculated for each replicate.

492

493   **OPP-staining and translational activity measurement.**

494   Click-iT Plus OPP Alexa Fluor™ 488 Protein Synthesis Kit (Invitrogen) was used to label

495   *S. aureus* with O-propargyl-puromycin (OPP) following the manufacturer's instructions.

496   Briefly, 450 µl of bacteria exposed to pH 5.5 for 3 days were washed with PBS and resuspended

497   in pre-warmed TSB supplemented with 20 µM OPP. Labelling was performed at 37°C and 220

498   rpm shaking for 20 min. All subsequent steps were performed at room temperature. After

499   incubation, bacteria were washed with PBS and fixed in 3.7% formalin for 15 min. To

500   permeabilize the bacteria, fixative was removed, and bacteria were incubated in 100 µl of 0.5%

501   Triton X-100 in PBS for 15 min. After washing twice with PBS, bacteria were labelled using

502   1X Click-iT cocktail for 30 min in the dark. Bacteria were harvested and washed once with

503   Click-iT rinse buffer and resuspended in 40 µl of PBS for imaging or 150 µl of PBS for

504   fluorescence measurement on a SpectraMax i3 MiniMax 300 plate reader in white 96-well flat

505   bottom plates.

506

507   **LC-MS/MS**

508   **Proteomics sample preparation.**

509   A total of 12 samples (4 biological replicates for each strain) were processed for mass

510   spectrometry-based proteomics analysis. To extract the proteins, 30 µl SDS-lysis buffer [4%

511   (w/v) SDS, 100mM Tris-HCl pH 8.2, 0.1M dithiothreitol complemented with Halt Protease and

512   Phosphatase Inhibitor (Thermo Fisher Scientific)] was added to the frozen cell pellets. Samples

513   were mechanically lysed with glass beads in a tissue lyser (QIAGEN) for 4 cycles of 2 min,

514   running at 30 Hz. Between the cycles, samples were cooled down on ice. After spinning down

515   the samples, samples were boiled for 5 min at 95°C and placed 1 min in high-intensity focused

516   ultrasound sonication at 100% amplitude, 80% cycle (UP200St with VialTweeter, Hielscher

517   Ultrasound Technology). Samples were then diluted with 200 µl 8 M urea, 100 mM Tris-HCl

518   (pH 8.2) and centrifugated for 10 min at 8,000g at 4°C. The clear supernatant was transferred

519   into a new tube. Protein concentration was estimated with Qbit measurement (Invitrogen,

520   California, USA). Prior filter-aided sample preparation (FASP) [62], protein extracts were

521   incubated for 45 min with 1%v/v Benzonase Nuclease (SIGMA E1014). For the FASP

522   digestion, the clear protein lysate was deposited in a Microcon-30kDa filter unit (Millipore,

523   MRCF0R030) and centrifuged at 14,000g for 20 min to pass the totality of the sample through

524   the filter. After a wash step with 200 µl buffered urea [8 M urea, 100 mM Tris-HCl (pH 8.2)]

525   with the same centrifugation parameters as above, samples were incubated for 10 min with 50

526   mM iodoacetamide. The filter units were subsequently washed with 3 x 100 µl urea and 2x 100

527   µl 50 mM triethylammonium bicarbonate (TEAB). For overnight digestion at room

528   temperature, sample-filters were incubated in a wet-cell adding 1:50 w/w trypsin: protein ratio

529   (Promega, V5111) solubilized in 120 µl 50 mM TEAB. The next day, peptides were recovered

530   by centrifugation and a small aliquot of 3 µl was taken for proteome analysis and diluted with

531   3% acetonitrile, 0.1% formic acid to 0.3 raw absorbance at 280 nm (NanoDrop, DeNovix).

532

Phosphopeptide enrichment.

534   For ferric-nitrilotriacetate (Fe-NTA) phosphoenrichment, tryptic peptides were first dried in an

535   ultra-vacuum centrifugation. Then, equal amounts for each sample (600 µg based on protein

536   estimation) were enriched by Fe-NTA spin columns (Thermo Fisher Scientific, A32992)

537   following the provided instructions. Dried phosphopeptides were re-dissolved in 10 µl 3%

538   acetonitrile, 0.1% formic acid for mass spectrometry (MS) injections.

539

540 **Mass spectrometry.**

541 MS analyses were performed on an ACQUITY UPLC M-Class System (waters) coupled to an

542 Orbitrap Fusion Lumos (Thermo Fisher). For LC-MS/MS injections of proteome and

543 phosphoproteome samples, 2 µl and 4 µl, respectively, were loaded on a trap column [nanoEase

544 M/Z Symmetry C18 100 A, 5um, 1/PK 180 um x 20 mm (waters)] and separated on the

545 analytical column [nanoEase M/Z HSS C18 T3 Col 100 A, 1.8 um, 1 P/K 75 um x 250 mm

546 (waters)] using a linear gradient of 5-24% - 24-36% acetonitrile (0.1% formic acid) over 90

547 min (80 min – 10 min step) followed by an 20 min re-equilibration time. The analytical column

548 was temperature controlled at 50°C and the flow rate of 300 nL/min was constant over the

549 chromatographic separation.

550 MS survey scan from m/z 300-1500 were acquired at a resolution of 120,000 at m/z 200 in

551 profile mode, while tandem mass spectra were acquired in the IonTrap in centroid mode. For

552 HCD fragmentation, a normalized collision energy of 35 was applied and isolation windows of

553 m/z 0.8 (proteome) or m/z 1.2 (phosphoproteome) were used for MS2 acquisitions. The AGC

554 target was set to 10e5 for both types of samples, whereas the maximum injection time was

555 either 50 ms (proteome) or 120 ms (phosphoproteome). The mass spectrometry proteomics data

556 have been deposited to the ProteomeXchange Consortium via the PRIDE [63] partner repository

557 with the dataset identifier PXD025124.

558

559 **Protein identification and quantification.**

560 Peptide and protein identification/quantification were performed using label free quantification

561 and match between run option in MaxQuant (version 1.6.2.3). Spectra were searched against

562 the Uniprot *Staphylococcus aureus* reference database (downloaded 20201127), searching for

563 the variable modifications Acetylation (Protein N-term), Oxidation (M) and if applicable

564 Phosphorylation (STY) at 1% false discovery rate. For the proteome analyses, protein intensity

565 estimates were used as reported in the proteinGroups.txt file. For quantification, only protein

566   groups with at least two peptides were kept. For the phosphoproteome, the Maxquant output

567   reported in the "Phospho STY Sites.txt" was used. Intensities were normalized to systematically

568   remove variability in abundance due to different sample loads on the LC column. The $\log_2$

569   transformed intensities were z-scored, updated by the average of the standard deviation in all

570   samples. After normalization, all samples had a similar intensity distribution for computing a

571   moderated t-test [64], employing the R package limma [65]. All these functions are implemented in

572   the R package SRMService [66]. Pathway information of proteins was retrieved from the Kyoto

573   Encyclopedia of Genes and Genomes (KEGG) database [67] for visualization purposes.

574

575   **Immunoblotting.**

576   Bacterial total protein was isolated by bacterial lysis using glass beads. Briefly, bacteria were

577   washed twice with ice-cold PBS and resuspended in ice-cold PBS supplemented with 1X Halt

578   Protease and Phosphatase Inhibitor (Thermo Fisher Scientific). Bacteria were mechanically

579   lysed with glass beads in a tissue lyser (QIAGEN) for 3 cycles of 1.5 min, running at 30 Hz.

580   Between the cycles, samples were cooled down on ice. Cell debris and intact cells were

581   removed by centrifugation (1,200 g for 10 min at 4°C). Protein concentration was determined

582   by Bradford assay [68]. 10 µg of total protein were separated by sodium dodecyl sulphate

583   polyacrylamide gel electrophoresis (SDS-PAGE) (10% acrylamide) and transferred onto a

584   nitrocellulose membrane. Membranes were stained for total protein using the Novex™

585   Reversible Membrane Protein Stain Kit (Invitrogen) following the manufacturer's instructions.

586   After de-staining, membranes were blocked using 4% bovine serum albumin (BSA, Sigma) in

587   Tris-buffered saline for 2 h at room temperature. An antibody recognizing phospho-Threonine

588   (Cell Signaling, Phospho-Threonine (42H4) Mouse mAb #9386) was used to detect Thr-

589   phosphorlyation and a polyclonal rabbit serum was used to detect the translational elongation

590   factor EF-G, both from *S. aureus* and *B. subtilis*. Visualizing was performed using IRDye

591   secondary antibodies (LI-COR) and the Fusion FX6 EDGE Imaging System (Vilber Lourmat

592   S.A.).

593

594   **Statistical analysis.**

595   All experiments, except proteomics data, were analysed for statistical significance by either the

596   Kruskal-Wallis test with Dunn`s post-test, by one-way or two-way ANOVA with Tukey post-

597   test after normality testing by the Shapiro-Wilk normality test, unless otherwise indicated.

598   P-values are shown were appropriate. Analysis of proteomics data is explained in the mass

599   spectrometry section.

600

601   **Data availability.**

602   Raw data have been deposited in PRIDE [63]: PXD025124 and are publicly available. All other

603   study data are included in this article and supporting information.

Acknowledgement

References

614

615 1   Lowy, F. D. Staphylococcus aureus infections. *N Engl J Med* **339**, 520-532,
616   doi:10.1056/NEJM199808203390806 (1998).
617 2   Gorwitz, R. J. Understanding the success of methicillin-resistant Staphylococcus aureus
618   strains causing epidemic disease in the community. *J Infect Dis* **197**, 179-182,
619   doi:10.1086/523767 (2008).
620 3   Turner, N. A. *et al.* Methicillin-resistant Staphylococcus aureus: an overview of basic
621   and clinical research. *Nat Rev Microbiol* **17**, 203-218, doi:10.1038/s41579-018-0147-4
622   (2019).
623 4   Lowy, F. D. Antimicrobial resistance: the example of Staphylococcus aureus. *The*
624   *Journal of Clinical Investigation* **111**, 1265-1273, doi:10.1172/JCI18535 (2003).
625 5   Huemer, M., Mairpady Shambat, S., Brugger, S. D. & Zinkernagel, A. S. Antibiotic
626   resistance and persistence—Implications for human health and treatment
627   perspectives. *EMBO reports* **21**, e51034,
628   doi:https://doi.org/10.15252/embr.202051034 (2020).
629 6   Kahl, B. *et al.* Persistent infection with small colony variant strains of Staphylococcus
630   aureus in patients with cystic fibrosis. *J Infect Dis* **177**, 1023-1029, doi:10.1086/515238
631   (1998).
632 7   Proctor, R. A. *et al.* Small colony variants: a pathogenic form of bacteria that facilitates
633   persistent and recurrent infections. *Nat Rev Microbiol* **4**, 295-305,
634   doi:10.1038/nrmicro1384 (2006).
635 8   Conlon, B. P. Staphylococcus aureus chronic and relapsing infections: Evidence of a
636   role for persister cells. *BioEssays* **36**, 991-996, doi:10.1002/bies.201400080 (2014).
637 9   Balaban, N. Q. *et al.* Definitions and guidelines for research on antibiotic persistence.
638   *Nat Rev Microbiol* **17**, 441-448, doi:10.1038/s41579-019-0196-3 (2019).
639 10 Ackermann, M. A functional perspective on phenotypic heterogeneity in
640   microorganisms. *Nat Rev Microbiol* **13**, 497-508, doi:10.1038/nrmicro3491 (2015).
641 11 Claudi, B. *et al.* Phenotypic Variation of Salmonella in Host Tissues Delays Eradication
642   by Antimicrobial Chemotherapy. *Cell* **158**, 722-733,
643   doi:https://doi.org/10.1016/j.cell.2014.06.045 (2014).
644 12 Rowe, S. E. *et al.* Reactive oxygen species induce antibiotic tolerance during systemic
645   Staphylococcus aureus infection. *Nature Microbiology* **5**, 282-290,
646   doi:10.1038/s41564-019-0627-y (2020).
647 13 Vulin, C., Leimer, N., Huemer, M., Ackermann, M. & Zinkernagel, A. S. Prolonged
648   bacterial lag time results in small colony variants that represent a sub-population of
649   persisters. *Nat Commun* **9**, 4074, doi:10.1038/s41467-018-06527-0 (2018).
650 14 Peyrusson, F. *et al.* Intracellular Staphylococcus aureus persisters upon antibiotic
651   exposure. *Nature Communications* **11**, 2200, doi:10.1038/s41467-020-15966-7 (2020).
652 15 Levin, B. R. *et al.* A Numbers Game: Ribosome Densities, Bacterial Growth, and
653   Antibiotic-Mediated Stasis and Death. *mBio* **8**, doi:10.1128/mBio.02253-16 (2017).
654 16 Balaban, N. Q., Merrin, J., Chait, R., Kowalik, L. & Leibler, S. Bacterial persistence as a
655   phenotypic switch. *Science* **305**, 1622-1625, doi:10.1126/science.1099390 (2004).
656 17 Manuse, S. *et al.* Bacterial persisters are a stochastically formed subpopulation of low-
657   energy cells. *PLOS Biology* **19**, e3001194, doi:10.1371/journal.pbio.3001194 (2021).
658 18 Kyriakis, J. M. In the beginning, there was protein phosphorylation. *J Biol Chem* **289**,
659   9460-9462, doi:10.1074/jbc.R114.557926 (2014).

660   19   Stock, A. M., Robinson, V. L. & Goudreau, P. N. Two-Component Signal Transduction.
661   *Annual Review of Biochemistry* **69**, 183-215, doi:10.1146/annurev.biochem.69.1.183
662   (2000).

663   20   Bakal, C. J. & Davies, J. E. No longer an exclusive club: eukaryotic signalling domains in
664   bacteria. *Trends in Cell Biology* **10**, 32-38, doi:https://doi.org/10.1016/S0962-
665   8924(99)01681-5 (2000).

666   21   Garnak, M. & Reeves, H. C. Phosphorylation of Isocitrate dehydrogenase of Escherichia
667   coli. *Science* **203**, 1111-1112, doi:10.1126/science.34215 (1979).

668   22   Donat, S. *et al.* Transcriptome and Functional Analysis of the Eukaryotic-Type
669   Serine/Threonine Kinase PknB in Staphylococcus aureus. *Journal of Bacteriology* **191**,
670   4056, doi:10.1128/JB.00117-09 (2009).

671   23   Lomas-Lopez, R., Paracuellos, P., Riberty, M., Cozzone, A. J. & Duclos, B. Several
672   enzymes of the central metabolism are phosphorylated in Staphylococcus aureus.
673   *FEMS Microbiology Letters* **272**, 35-42, doi:10.1111/j.1574-6968.2007.00742.x (2007).

674   24   Hardt, P. *et al.* The cell wall precursor lipid II acts as a molecular signal for the Ser/Thr
675   kinase PknB of Staphylococcus aureus. *Int J Med Microbiol* **307**, 1-10,
676   doi:10.1016/j.ijmm.2016.12.001 (2017).

677   25   Truong-Bolduc, Q. C., Ding, Y. & Hooper, D. C. Posttranslational modification influences
678   the effects of MgrA on norA expression in Staphylococcus aureus. *J Bacteriol* **190**,
679   7375-7381, doi:10.1128/jb.01068-08 (2008).

680   26   Tamber, S., Schwartzman, J. & Cheung, A. L. Role of PknB kinase in antibiotic resistance
681   and virulence in community-acquired methicillin-resistant Staphylococcus aureus
682   strain USA300. *Infect Immun* **78**, 3637-3646, doi:10.1128/IAI.00296-10 (2010).

683   27   Passalacqua, K. D., Satola, S. W., Crispell, E. K. & Read, T. D. A Mutation in the PP2C
684   Phosphatase Gene in Staphylococcus aureus USA300 Clinical Isolate with Reduced
685   Susceptibility to Vancomycin and Daptomycin. *Antimicrobial Agents and*
686   *Chemotherapy* **56**, 5212, doi:10.1128/AAC.05770-11 (2012).

687   28   Sun, F. *et al.* Protein cysteine phosphorylation of SarA/MgrA family transcriptional
688   regulators mediates bacterial virulence and antibiotic resistance. *Proceedings of the*
689   *National Academy of Sciences* **109**, 15461-15466, doi:10.1073/pnas.1205952109
690   (2012).

691   29   Burnside, K. *et al.* Regulation of Hemolysin Expression and Virulence of Staphylococcus
692   aureus by a Serine/Threonine Kinase and Phosphatase. *PLOS ONE* **5**, e11071,
693   doi:10.1371/journal.pone.0011071 (2010).

694   30   Débarbouillé, M. *et al.* Characterization of a Serine/Threonine Kinase Involved in
695   Virulence of Staphylococcus aureus. *Journal of Bacteriology* **191**, 4070,
696   doi:10.1128/JB.01813-08 (2009).

697   31   Ohlsen, K. & Donat, S. The impact of serine/threonine phosphorylation in
698   Staphylococcus aureus. *Int J Med Microbiol* **300**, 137-141,
699   doi:10.1016/j.ijmm.2009.08.016 (2010).

700   32   Diez, S., Ryu, J., Caban, K., Gonzalez, R. L. & Dworkin, J. The alarmones (p)ppGpp
701   directly regulate translation initiation during entry into quiescence. *Proceedings of the*
702   *National Academy of Sciences* **117**, 15565-15572, doi:10.1073/pnas.1920013117
703   (2020).

704   33   Pereira, S. F., Gonzalez, R. L., Jr. & Dworkin, J. Protein synthesis during cellular
705   quiescence is inhibited by phosphorylation of a translational elongation factor. *Proc*
706   *Natl Acad Sci U S A* **112**, E3274-3281, doi:10.1073/pnas.1505297112 (2015).

34   Nekoofar, M. H. *et al.* pH of pus collected from periapical abscesses. *Int Endod J* **42**, 534-538, doi:10.1111/j.1365-2591.2009.01550.x (2009).

35   Leimer, N. *et al.* Nonstable Staphylococcus aureus Small-Colony Variants Are Induced by Low pH and Sensitized to Antimicrobial Therapy by Phagolysosomal Alkalinization. *J Infect Dis* **213**, 305-313, doi:10.1093/infdis/jiv388 (2016).

36   Häffner, N. *et al.* Intracellular Environment and agr System Affect Colony Size Heterogeneity of Staphylococcus aureus. *Front Microbiol* **11**, 1415, doi:10.3389/fmicb.2020.01415 (2020).

37   Liebeke, M., Meyer, H., Donat, S., Ohlsen, K. & Lalk, M. A metabolomic view of Staphylococcus aureus and its ser/thr kinase and phosphatase deletion mutants: involvement in cell wall biosynthesis. *Chem Biol* **17**, 820-830, doi:10.1016/j.chembiol.2010.06.012 (2010).

38   Huemer, M. *et al.* Molecular reprogramming and phenotype switching in Staphylococcus aureus lead to high antibiotic persistence and affect therapy success. *Proceedings of the National Academy of Sciences* **118**, e2014920118, doi:10.1073/pnas.2014920118 (2021).

39   Prust, N., van der Laarse, S. A. M., van den Toorn, H., van Sorge, N. M. & Lemeer, S. In depth characterization of the Staphylococcus aureus phosphoproteome reveals new targets of Stk1. *Molecular & Cellular Proteomics*, mcp.RA120.002232, doi:10.1074/mcp.RA120.002232 (2020).

40   Liu, J., Xu, Y., Stoleru, D. & Salic, A. Imaging protein synthesis in cells and tissues with an alkyne analog of puromycin. *Proceedings of the National Academy of Sciences* **109**, 413-418, doi:10.1073/pnas.1111561108 (2012).

41   De Lencastre, H. *et al.* Antibiotic Resistance As a Stress Response: Complete Sequencing of a Large Number of Chromosomal Loci in Staphylococcus aureus Strain COL That Impact on the Expression of Resistance to Methicillin. *Microbial Drug Resistance* **5**, 163-175, doi:10.1089/mdr.1999.5.163 (1999).

42   Beltramini, A. M., Mukhopadhyay, C. D. & Pancholi, V. Modulation of cell wall structure and antimicrobial susceptibility by a Staphylococcus aureus eukaryote-like serine/threonine kinase and phosphatase. *Infect Immun* **77**, 1406-1416, doi:10.1128/IAI.01499-08 (2009).

43   Jarick, M. *et al.* The serine/threonine kinase Stk and the phosphatase Stp regulate cell wall synthesis in Staphylococcus aureus. *Sci Rep* **8**, 13693, doi:10.1038/s41598-018-32109-7 (2018).

44   Kant, S., Asthana, S., Missiakas, D. & Pancholi, V. A novel STK1-targeted small-molecule as an "antibiotic resistance breaker" against multidrug-resistant Staphylococcus aureus. *Sci Rep* **7**, 5067, doi:10.1038/s41598-017-05314-z (2017).

45   Talavera, A. *et al.* Phosphorylation decelerates conformational dynamics in bacterial translation elongation factors. *Sci Adv* **4**, eaap9714, doi:10.1126/sciadv.aap9714 (2018).

46   Kwan, B. W., Valenta, J. A., Benedik, M. J. & Wood, T. K. Arrested protein synthesis increases persister-like cell formation. *Antimicrob Agents Chemother* **57**, 1468-1473, doi:10.1128/AAC.02135-12 (2013).

47   Song, S. & Wood, T. K. ppGpp ribosome dimerization model for bacterial persister formation and resuscitation. *Biochem Biophys Res Commun* **523**, 281-286, doi:10.1016/j.bbrc.2020.01.102 (2020).

33

48   Maurya, G. K. *et al.* Phosphorylation of FtsZ and FtsA by a DNA Damage-Responsive Ser/Thr Protein Kinase Affects Their Functional Interactions in Deinococcus radiodurans. *mSphere* **3**, doi:10.1128/mSphere.00325-18 (2018).

49   Thakur, M. & Chakraborti, P. K. GTPase activity of mycobacterial FtsZ is impaired due to its transphosphorylation by the eukaryotic-type Ser/Thr kinase, PknA. *J Biol Chem* **281**, 40107-40113, doi:10.1074/jbc.M607216200 (2006).

50   Manuse, S., Fleurie, A., Zucchini, L., Lesterlin, C. & Grangeasse, C. Role of eukaryotic-like serine/threonine kinases in bacterial cell division and morphogenesis. *FEMS Microbiology Reviews* **40**, 41-56, doi:10.1093/femsre/fuv041 (2015).

51   Yu, J., Liu, Y., Yin, H. & Chang, Z. Regrowth-delay body as a bacterial subcellular structure marking multidrug-tolerant persisters. *Cell Discovery* **5**, 8, doi:10.1038/s41421-019-0080-3 (2019).

52   Levin-Reisman, I., Fridman, O. & Balaban, N. Q. ScanLag: high-throughput quantification of colony growth and lag time. *J Vis Exp*, doi:10.3791/51456 (2014).

53   Conlon, B. P. *et al.* Persister formation in Staphylococcus aureus is associated with ATP depletion. *Nat Microbiol* **1**, 16051, doi:10.1038/nmicrobiol.2016.51 (2016).

54   Shan, Y. *et al.* ATP-Dependent Persister Formation in Escherichia coli. *mBio* **8**, doi:10.1128/mBio.02267-16 (2017).

55   Pu, Y. *et al.* ATP-Dependent Dynamic Protein Aggregation Regulates Bacterial Dormancy Depth Critical for Antibiotic Tolerance. *Mol Cell* **73**, 143-156.e144, doi:https://doi.org/10.1016/j.molcel.2018.10.022 (2019).

56   Lukat, G. S., McCleary, W. R., Stock, A. M. & Stock, J. B. Phosphorylation of bacterial response regulator proteins by low molecular weight phospho-donors. *Proc Natl Acad Sci U S A* **89**, 718-722, doi:10.1073/pnas.89.2.718 (1992).

57   Wolfe, A. J. Physiologically relevant small phosphodonors link metabolism to signal transduction. *Curr Opin Microbiol* **13**, 204-209, doi:10.1016/j.mib.2010.01.002 (2010).

58   Vornhagen, J. *et al.* Kinase Inhibitors that Increase the Sensitivity of Methicillin Resistant Staphylococcus aureus to beta-Lactam Antibiotics. *Pathogens* **4**, 708-721, doi:10.3390/pathogens4040708 (2015).

59   Monk, I. R., Shah, I. M., Xu, M., Tan, M. W. & Foster, T. J. Transforming the untransformable: application of direct transformation to manipulate genetically Staphylococcus aureus and Staphylococcus epidermidis. *MBio* **3**, doi:10.1128/mBio.00277-11 (2012).

60   Ford, C. W., Hamel, J. C., Stapert, D. & Yancey, R. J. Establishment of an experimental model of a Staphylococcus aureus abscess in mice by use of dextran and gelatin microcarriers. *J Med Microbiol* **28**, 259-266, doi:10.1099/00222615-28-4-259 (1989).

61   Malachowa, N., Kobayashi, S. D., Braughton, K. R. & DeLeo, F. R. Mouse model of Staphylococcus aureus skin infection. *Methods Mol Biol* **1031**, 109-116, doi:10.1007/978-1-62703-481-4_14 (2013).

62   Wiśniewski, J. R., Zougman, A., Nagaraj, N. & Mann, M. Universal sample preparation method for proteome analysis. *Nat Methods* **6**, 359-362, doi:10.1038/nmeth.1322 (2009).

63   Perez-Riverol, Y. *et al.* The PRIDE database and related tools and resources in 2019: improving support for quantification data. *Nucleic Acids Res* **47**, D442-D450, doi:10.1093/nar/gky1106 (2019).

64   Smyth, G. K. Linear models and empirical bayes methods for assessing differential expression in microarray experiments. *Stat Appl Genet Mol Biol* **3**, Article3, doi:10.2202/1544-6115.1027 (2004).

801   65   Ritchie, M. E. *et al.* limma powers differential expression analyses for RNA-sequencing
802   and microarray studies. *Nucleic Acids Res* **43**, e47, doi:10.1093/nar/gkv007 (2015).

803   66   Wolski, W., Grossmann, J. & Panse, C. *R Package for Reporting of Quantitative Mass*
804   *Spectrometry Data.*, 2018).

805   67   Kanehisa, M. & Goto, S. KEGG: kyoto encyclopedia of genes and genomes. *Nucleic*
806   *Acids Res* **28**, 27-30, doi:10.1093/nar/28.1.27 (2000).

807   68   Bradford, M. M. A rapid and sensitive method for the quantitation of microgram
808   quantities of protein utilizing the principle of protein-dye binding. *Anal Biochem* **72**,
809   248-254, doi:10.1006/abio.1976.9999 (1976).

810